

# First Principle Study of Ethanol Adsorption and Formation of Hydrogen Bond on Rh(111) Surface

Ming-Mei Yang,<sup>†,‡</sup> Xin-He Bao,<sup>\*,†</sup> and Wei-Xue Li<sup>\*,†,§</sup>

State Key Laboratory of Catalysis, Dalian Institute of Chemical Physics, Chinese Academy of Sciences, Dalian, 116023, China, Center for Theoretical and Computational Chemistry, Dalian Institute of Chemical Physics, Chinese Academy of Sciences, Dalian, 116023, China, and Graduate School of the Chinese Academy of Sciences, Beijing, 100039, China

Received: December 15, 2006; In Final Form: March 9, 2007

Density functional theory (DFT) calculations are performed to study the ethanol adsorption on Rh(111) surfaces. Various adsorption modes, including monomer, dimer, and one-dimensional (1D) chain, are investigated and analyzed in details from energetic, geometrical, vibrational, and electronic points of view, which lead to valuable insights into alcohol molecules adsorption on metal surfaces. It is found that ethanol molecules prefer to adsorb at atop sites and bind to the surfaces through the oxygen atom, independent of the coverage and adsorption modes. The adsorption is exothermic, and the average adsorption energy is  $-0.5$  eV per molecule. Adsorbed ethanol molecules are energetically favorable to agglomerate to dimer and chain by formation of the hydrogen bond. The ethanol adsorption induces significant red shift of the hydroxyl stretching vibration ( $\nu(\text{OH})$ ). It is found that the red shifts are very sensitive to the coverage and adsorption modes. Depending on the nature of the H-bond, be it H-acceptor or H-donor sharing, there is a distinct pair of  $\nu(\text{OH})$  vibration, which can be seen as the fingerprint of the existence of hydroxyl-contained molecules and the formation of the H-bond. Our results show that the interaction between adsorbate and substrate and the H-bonding between adsorbed ethanol molecules can result in the overall red shift of  $\nu(\text{OH})$  to the magnitude of  $769\text{ cm}^{-1}$ .

## 1. Introduction

With the globally declining petrochemical reserves, alcohols are one of the most renewable resources for hydrogen production in fuel cell applications and, therefore, have attracted extensive attention recently. It has been reported that ethanol and ethanol–water mixtures can be converted directly into  $\text{H}_2$  with  $\sim 100\%$  selectivity and  $>95\%$  conversion by catalytic partial oxidation on rhodium–ceria catalysts.<sup>1</sup> The study of alcohol adsorption, decomposition, and oxidation is also important to identify the possible intermediates during the Fischer–Tropsch synthesis of alcohols from syngas ( $\text{CO}$  and  $\text{H}_2$ ).<sup>2</sup> Despite the numerous studies conducted so far, microscopic understanding of the chemistry between ethanol and catalyst in terms of energetics and geometries remains unclear.

In the past, alcohol and water molecules in solvent have been studied and well documented in literatures.<sup>3–11</sup> One of distinct features found in these studies is the existence of H-bond via hydroxyl groups between alcohol molecules and its significant effect on the reactivity and vibrations etc. The heterogeneity present at the liquid/solid or air/solid interfaces may however provide certain constraint to the formation of the H-bond between adsorbed alcohol molecules. On the other hand, the H-bonding between alcohol molecules may compete with the bonding between alcohol molecules and metal surfaces. The interplay of these two types of interactions and their

dependence on the substrates, which determines the general behavior of wetting or clustering of the alcohol molecules on metal surfaces, are critical to the reactivity and selectivity of alcohol chemistry on metal surfaces, which will be addressed in present work.

Ethanol adsorption and decomposition on metal surfaces, including Ni(111),<sup>12</sup> Ni(100),<sup>13</sup> Rh(100),<sup>14</sup> Rh(111),<sup>15–17</sup> Pt(111),<sup>18–20</sup> Pt(331),<sup>21,22</sup> and Pd(110),<sup>23,24</sup> have been studied by X-ray photoelectron spectroscopy (XPS), thermal desorption spectroscopy (TDS), infrared reflection absorption spectroscopy (IRAS), and high-resolution electron energy loss spectroscopy (HREELS). For submonolayer coverage on closely packed (111) surfaces, it has been found that ethanol molecules bond to the surface through the oxygen atom, where the corresponding O–H bonds are nearly parallel to the surface. On these surfaces, the ethanol adsorption was seen to saturate at 0.2 ML on Ni(111),<sup>12</sup> 0.44 ML on Pt(111),<sup>18</sup> after which it would form multilayer for further exposure. For ethanol adsorption on the Rh(111) surface, HREELS data show that both of the O–H bending ( $\gamma(\text{OH})$ ) and stretching modes ( $\nu(\text{OH})$ ) were softened: the  $\nu(\text{OH})$  mode ( $3660\text{ cm}^{-1}$  in gas phase) occurred at  $3270\text{ cm}^{-1}$  and the  $\gamma(\text{OH})$  mode ( $1241\text{ cm}^{-1}$  in gas phase) at  $815\text{ cm}^{-1}$  upon adsorption.<sup>16</sup> From XPS measurements, two C1s peaks have been identified, were found to shift toward higher energy with increasing coverage, and were attributed to the multilayer growth.<sup>17</sup> Using TDS, two ethanol desorption peaks on the Rh(111) surface were observed in the temperature range of  $220\text{--}260\text{ K}$ ,<sup>2</sup> which is accompanied with the dissociation.<sup>17</sup> So far, theoretical studies has been mainly limited to the methanol, whose adsorption and decomposition on metal surfaces have been studied experimentally and theoretically.<sup>25–38</sup>

\* To whom correspondence should be addressed. E-mail: wxli@dicp.ac.cn, xhbao@dicp.ac.cn.

<sup>†</sup> State Key Laboratory of Catalysis, Dalian Institute of Chemical Physics.

<sup>‡</sup> Graduate School of the Chinese Academy of Sciences.

<sup>§</sup> Center for Theoretical and Computational Chemistry, Dalian Institute of Chemical Physics.

In these studies, the energetics, geometry and vibration as well as the formation of the H-bond between adsorbed methanol molecules have been studied. Theoretical studies on ethanol are less explored; yet until now, only ethanol adsorption and dissociation on Pt (111) surface have been investigated by Dumesic and co-workers recently.<sup>20</sup>

The present paper focuses on the ethanol adsorption on Rh(111) surface, as a model system, and studied within the submonolayer regime using DFT. Computational details are described in Section 2. The main results for ethanol adsorption and formation of the H-bond on Rh(111) are presented in Section 3. Ethanol monomer, dimer, and one-dimensional (1D) chains have been studied in terms of structure, energetics, and vibration, which provide valuable insight on the interaction between adsorbate and substrate and lateral interaction between adsorbates. The effect of the H-bond on the geometries, electronic properties, and vibrations has been analyzed. In Sections 4 and 5, a comparison with available experimental data and electronic analysis, respectively, are given. A brief summary is given in Section 6.

## 2. Computation Methods

Density functional theory calculations were performed using DACAPO package,<sup>39</sup> where ultrasoft-pseudopotentials were employed to describe the ion cores. The Kohn–Sham one-electron valence states are expanded in a basis of plane waves with kinetic energies up to 25 Ry. The exchange-correlation energy and potential are approximated by generalized gradient functional self-consistently, GGA-PW91.<sup>40</sup> During iterative diagonalization of the Kohn–Sham Hamiltonian, Fermi population of the Kohn–Sham states ( $k_B T = 0.1$  eV) and Pulay mixing of the resulting electronic density are used to improve the convergence, such that the total energy can be extrapolated to absolute zero correspondingly.

The Rh(111) surface was represented by a three-layer slab separated by seven layer-equivalents of vacuum. Supercells with periodicity  $(\sqrt{3} \times \sqrt{3})$ ,  $(\sqrt{3} \times 2\sqrt{3})$ ,  $(\sqrt{3} \times 3\sqrt{3})$ , and  $(2 \times 2)$  were used to simulate adsorption of the ethanol monomer, dimer, and one-dimensional (1D) chain structures at different coverage. The  $k$ -point samplings in the Brillouin zone were  $(4 \times 4 \times 1)$  and  $(4 \times 2 \times 1)$  for supercells with  $(2 \times 2)$  and  $(\sqrt{3} \times 3\sqrt{3})$  periodicity, and adjusted accordingly when periodicity changes. The chemisorbed species and the atoms in the top metal layer were relaxed until the residual forces less than  $0.02$  eV/Å, while the atoms in the bottom two layers were frozen in bulk-truncated positions. The calculated lattice constant for bulk Rh is  $3.83$  Å, which agrees well with the experimental value of  $3.80$  Å, and has been employed throughout the paper. Calculations for the isolated gas-phase molecules were carried out in a  $15.0 \times 15.25 \times 15.5$  Å unit cell and the Brillouin zone was sampled with one  $k$  point. Spin-polarization was included during the optimization for gas-phase radical species. Adsorbates were placed on one side of the slab, where a dipole correction has been applied to remove the artificial interaction by the presence of nonequivalent surfaces.<sup>41</sup>

The vibrations of ethanol were calculated on the basis of the numerical calculations of the second derivatives of the potential energy surface within the harmonic approach by diagonalization of the force constant matrix, built with finite differences of the first derivatives of the total energies by geometrical perturbations of the optimized Cartesian coordinates of the system.<sup>42</sup> Because the force constants were sensitive to the structures, it was optimized until the residual forces were less than  $0.01$  eV/Å for all of the vibration calculations. The perturbation displace-

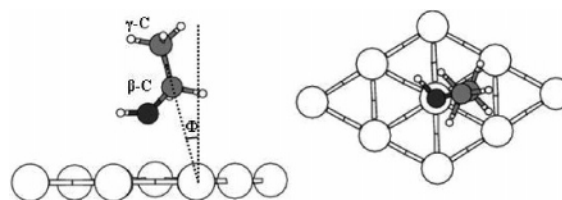


**Figure 1.** The schematic plot for ethanol monomer adsorption on Rh(111) surface (side view (left) and top view (right)). Dark gray for oxygen, lighter gray for carbon, and small white for hydrogen.  $\Phi$  is the angle between C–C bond and the surface normal direction.

ments were chosen to be  $0.02$  Å during the calculation of the force constants to maintain the harmonic approximation.

The averaged adsorption energy,  $E_{\text{ads}}^N$ , with  $N$  ethanol molecules in the supercell, is defined as

$$E_{\text{ads}}^N = (E_{\text{eth/M}}^N - N \times E_{\text{eth}} - E_M)/N \quad (1)$$

where  $E_{\text{eth/M}}^N$  is the total energy of the adsorbed-substrate system,  $E_M$  is the total energy of the bare metal slab, and  $E_{\text{eth}}$  is the total energy of isolated ethanol molecule in gas phase. Here, a negative  $E_{\text{ads}}^N$  means the adsorption is exothermic.

## 3. Results

The calculated energetics, geometries, vibrational frequencies of ethanol molecules on Rh(111), and its dependence on coverage are studied in this section. The agglomeration of adsorbed ethanol molecules and dimer and chain structures, are then considered.

**3.1. Ethanol Monomer Adsorption.** To validate the computational setup, a free gas-phase molecule was first studied. There are two stable conformers of ethanol molecule, *trans*- and *cis-gauche*, which are nearly isoenergetic (as confirmed by our calculations) and can interconvert by the torsion of the hydroxyl group from the ethyl mirror plane.<sup>43,44</sup> For *trans*-ethanol, calculated bond lengths for O–H, C–O, and C–C bond and angle for C–C–O are  $0.98$ ,  $1.43$ , and  $1.52$  Å and  $113.1^\circ$ , respectively. These results agree well with experimental values of  $0.97$ ,  $1.43$ , and  $1.51$  Å and  $107.8^\circ$ . Similar results have been reported by Dumesic and co-workers using the same code.<sup>20</sup>

For monomer adsorption on Rh(111) surface, the structures are optimized within  $(\sqrt{3} \times 3\sqrt{3})$ ,  $(\sqrt{3} \times 2\sqrt{3})$ ,  $(2 \times 2)$  and  $(\sqrt{3} \times \sqrt{3})$  supercells for coverage of  $1/9$ ,  $1/6$ ,  $1/4$ , and  $1/3$  ML, respectively. Among of them, the shortest atom (hydrogen) distance between adsorbates and their periodic images at  $1/3$  ML (highest coverage considered in the present work) is  $2.59$  Å, which is sufficient large to prevent possible chemical/hydrogen bonding formed through the periodic boundary and justify the monomer adsorption. Schematic structure is shown in Figure 1. From our calculations, it is found that ethanol molecules prefer to adsorb at atop sites and bind to the surfaces through the oxygen atom, irrespective to coverage. Adsorption at hollow site is unstable, and ethanol molecule displaces without barrier to atop site during the optimization. The calculated adsorption energies,  $E_{\text{ads}}^N$  and main geometric parameters are given in Table 1. We find that the interaction between ethanol and Rh surfaces is weak, and the averaged adsorption energy is  $-0.42$  eV at  $1/9$  ML. With an increase of ethanol coverage from  $1/9$  to  $1/3$  ML, the averaged adsorption energy decreases slightly ( $\sim 100$  meV) due to the steric repulsion. Correspondingly, the O–Rh bond length increases from  $2.32$  to  $2.43$  Å. Compared to ethanol molecules in the gas phase, where *cis*- and *trans-gauche* conformers are isoenergetic, adsorbed ethanol on

**TABLE 1: The Averaged Adsorption Energies  $E_{\text{ads}}$  for Monomer Adsorption (eV) and Corresponding Main Structural Parameters ( $\text{\AA}$  and degree), Vibrational Frequencies ( $\text{cm}^{-1}$ ), Variation of Work Function  $\Delta\varphi$  (eV), and Surface Dipole Moment  $\mu$  (Debye) at Different Coverage  $\theta$  (ML)**

$\theta$	$E_{\text{ads}}$	O–Rh	O–H	C–O	$\Phi$	$\nu_{\text{OH}}$	$\Delta\varphi$	$\mu$
1/9	-0.42	2.32	0.99	1.45	16.2	3656	-1.28	1.93
1/6	-0.39	2.34	0.99	1.45	16.3	3616	-1.62	1.63
1/4	-0.36	2.40	0.99	1.45	27.6	3518	-1.85	1.24
1/3	-0.32	2.43	0.99	1.45	13.7	3527	-2.07	1.04

Rh(111) is primarily *cis-gauche*, with the hydroxyl group pointing away from the ethyl mirror plane.

The weak adsorbate–surface interaction can be illustrated further by the modest variation of the structures of the ethanol molecule. For instance, the height of  $\beta$ -C (carbon atom bond directly to oxygen atom in OH group) is roughly 3.10  $\text{\AA}$  from the surface for various structures considered. It is found that methyl group can rotate along the C–C axis without any noticeable barrier. Compared to the free molecule in gas phase, the O–H and C–O bonds are elongated slightly by 0.01  $\text{\AA}$  and 0.02  $\text{\AA}$ , while the C–C bond shortens by 0.01  $\text{\AA}$ , and the angle for the C–C–O slightly decreases by  $2^\circ$ , irrespective of the coverage, as tabulated in Table 1. At coverage of 1/9 ML, the O–H bonds nearly parallel to the surface, where the angle between O–H bond and the (111) surface is  $1.74^\circ$  (upward). With increase of the coverage, the O–H bond points downward to the surface with angle  $2.89^\circ$ ,  $12.0^\circ$ , and  $13.2^\circ$  for coverage of 1/6, 1/4, and 1/3 ML, respectively. As seen in Figure 1, the C–C bond is tilted with respect to the normal direction of the surfaces represent as  $\Phi$ , listed in Table 1.

We now turn to the calculated vibrational frequencies for the adsorbed ethanol. For reference, the vibrations of the isolated gas-phase ethanol molecule are calculated first. The stretch frequency of the OH bond  $\nu(\text{OH}-)$ , methyl bond  $\nu(\text{CH}_3-)$  and the C–C–O bend  $\nu(\text{C}-\text{C}-\text{O})$  are 3863, 3088, and 1180  $\text{cm}^{-1}$ , respectively. Compared to the experimental values of 3660, 2965, and 1060  $\text{cm}^{-1}$ ,<sup>45</sup> our results are consistently 100–200  $\text{cm}^{-1}$  higher. Our calculations overestimate the stretch by about 5%, which is a typical error bar in DFT calculations.<sup>46,47</sup> For ethanol adsorption, the calculated  $\nu(\text{CH}_3-)$  and  $\nu(\text{C}-\text{C}-\text{O})$  vibrations at 1/4 ML are 3073 and 1220  $\text{cm}^{-1}$ , and the small difference from the gas phase are in line with the weak interaction between the adsorbates and the metal substrates. Accordingly, only the stretching frequencies  $\nu(\text{OH})$ , which bonds directly to the surface, are listed in Table 1 and discussed in the following sections.

Compared to the  $\nu(\text{OH})$  of the free ethanol, the adsorbed molecular vibration is softened by roughly 207  $\text{cm}^{-1}$  for a coverage of 1/9 ML, due to the coupling between adsorbed ethanol molecules and the substrate, as evidenced by the elongation of O–H bond length in above and charge depletion (seen Figure 5 given below). The softness (red shift) increases with the coverage, and our calculations show the largest red shift by 345  $\text{cm}^{-1}$  reached at the coverage of 1/3 ML.

Using HREELS, Houtman et al. found that for ethanol adsorption on the Rh(111) surface, the majority of the vibrational modes are lack of perturbation except the softness of O–H stretching modes.<sup>16</sup> The  $\nu(\text{OH})$  mode reported at 3660  $\text{cm}^{-1}$  in the gas phase was located at 3270  $\text{cm}^{-1}$  on the surface. On the basis of these measurements, they concluded that adsorbed ethanol molecules bonded to the surfaces via its oxygen atom. These findings agree qualitatively with the present calculations. There is, however, significant deviation with respect to the amount of the red shift of  $\nu(\text{OH})$ : 390  $\text{cm}^{-1}$  from the

measurement, and 207  $\text{cm}^{-1}$  from the present calculation at 1/9 ML. For ethanol adsorption at 1/3 ML, the red shift is 345  $\text{cm}^{-1}$ , which is closer to the experimental findings. However, as seen at below, ethanol tends to agglomerate to dimer and chain on metal surfaces, and the vibration assignment will be discussed further there.

**3.2. Ethanol Dimer Adsorption.** Ethanol molecules may bind with each other by the H-bond through its hydroxyl group. In gas phase, our calculations show that the H-bond formation is energetically favorable, and H-bond energy is calculated to be -130 meV per ethanol molecule or -260 meV per H-bond. Within the ethanol dimer, one ethanol molecule acts as the H-donor, with the OH group participating in the H-bond toward oxygen atom in the remained ethanol, which acts as H-acceptor. The O–O distance along the H-bond (O(H)···H) is 2.87  $\text{\AA}$ . Compared to the isolated monomer, main structural parameters of ethanol are intact, and only a slight elongation of O–H bond for the H-acceptor (0.01  $\text{\AA}$ ) and the H-donor (0.02  $\text{\AA}$ ), shortness of the C–O bond by 0.01  $\text{\AA}$  for the H-donor, and decrease of C–C–O angle by  $2^\circ$  for the H-acceptor are found.

The ethanol dimer are found to be energetically favorable on Rh(111) surface within ( $\sqrt{3} \times 3\sqrt{3}$ ) and ( $\sqrt{3} \times 2\sqrt{3}$ ) supercells, which correspond to coverage of 2/9 and 1/3 ML, respectively. Note that the dimer configuration is failed to form on ( $2 \times 2$ ) surface (corresponding to the coverage of 1/2 ML) due to the significant steric repulsion between the alkyls. Like monomer adsorption, two ethanol molecules within the dimer tend to maintain atop site preference, whenever it is possible. Two geometries with similar energetics are found in our calculations. For the previous one, both of the C–C bonds title away from the normal direction of the surface within  $31^\circ$ , as seen in Figure 2 and tabulated in Table 2, while for the later one, C–C bond almost parallels to the surface. The former one is energetically slightly favorable by 10 meV per ethanol molecules (though these may fall well in the numeric accuracy) at both 2/9 and 1/3 ML. For simplicity, only the former structure were studied and discussed in below. Though both of ethanol molecules within dimer prefer the atop sites, the height of two oxygen atoms in each of them are different, and corresponding vertical bucklings are 0.92 and 0.96  $\text{\AA}$  at 2/9 and 1/3 ML, respectively. Compared to the monomer adsorption, the height of oxygen atom of the lower-lying ethanol molecule (so-called H-donor) is 0.1  $\text{\AA}$  closer to the surface. The hydroxyl group in the H-donor points upward to oxygen atom of the H-acceptor (the higher-lying ethanol molecule), whose hydroxyl group points downward to the surface. Compared to the O–H bond length of the adsorbed monomer (0.99  $\text{\AA}$ ), the O–H bonds for both the H-donor and H-acceptor have been slightly stretched either by the participation into the H-bond or by the coupling with the substrate underneath. For adsorbed ethanol dimer, O–O distance along the H bond (O(H)···H) is 2.69  $\text{\AA}$ , which is 0.18  $\text{\AA}$  smaller with respect to the dimer in gas phase. This is because both ethanol molecules in the adsorbed dimer tend to maintain the atop site adsorption (accomplished by vertical buckling) of surface Rh atoms next to each other, whose position, however, is prevented by the neighbor Rh atoms. The main structural parameters are listed in Table 2.

The averaged adsorption energy (per ethanol) adsorption are given in Table 2, and they are -0.50 eV for 2/9 ML and -0.48 eV for 1/3 ML, in contrast to -0.42 and -0.39 eV for monomer adsorption with same periodicity (corresponding to coverages of 1/9 and 1/6ML, respectively). Calculated adsorption energy can be roughly divided into energy gain from the bonding between the dimer and substrate, and H-bonding between the

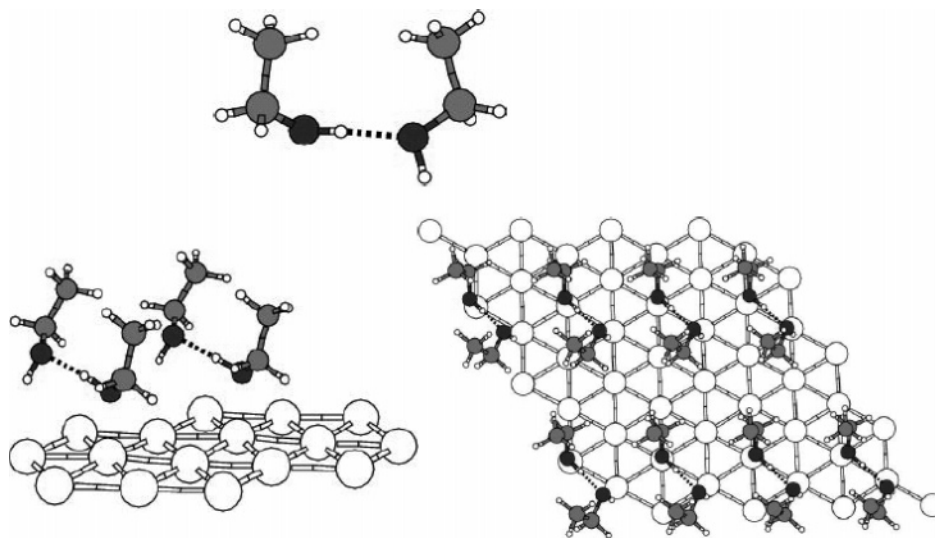


**Figure 2.** Optimized structures of ethanol dimer in gas phase (upper panel) and adsorption on Rh(111) surface (lower panel). Top view (left) and side view (right) have been shown, and only the first layer surface atoms are shown for clarity.

**TABLE 2: Averaged Adsorption Energies  $E_{\text{ads}}$ , H Bond Energy  $E_{\text{H-bond}}$  Per Molecule (eV) for Dimer Adsorption, and Corresponding Main Structure Parameters (Å and degree), Vibrational Frequencies ( $\text{cm}^{-1}$ ), Variation of Work Function  $\Delta\varphi$  (eV), and Surface Dipole Moment  $\mu$  (Debye) at Different Coverage  $\theta$  (ML)**

$\theta$	$E_{\text{ads}}$	$E_{\text{H-bond}}$	O–Rh	O–H	$O_a-O_b$	C–O	$\Phi$	$\nu_{\text{OH}}$	$\Delta\varphi$	$\mu$
gas phase				0.99	2.87	1.42		3618		
				0.98		1.44		3862		
2/9	−0.50	−0.127	2.22	1.01	2.69	1.44	19.5	3094	−1.37	1.03
			3.42	1.00		1.45	31.7	3448		
1/3	−0.48	−0.157	2.24	1.01	2.69	1.44	20.5	3119	−1.70	0.85
			3.45	1.00		1.44	29.2	3416		

ethanol molecules in dimer. As an approximation, the H-bond energy,  $E_{\text{H-bond}}$  (per ethanol), is calculated by

$$E_{\text{H-bond}} = (E_{2\text{eth}} - 2 \times E_{\text{eth}})/2 \quad (2)$$

where  $E_{2\text{eth}}$  is the total energy of frozen ethanol dimer taken from the optimized ethanol/substrate system in the same supercell but without the presence of the substrate, and  $E_{\text{eth}}$  is the total energy of isolated ethanol molecule in gas phase. Using eq 2, the calculated H-bond energies are  $-127$  meV/ethanol ( $-255$  meV/H-bond) for 2/9 ML and  $-157$  meV/ethanol ( $-315$  meV/H-bond) for 1/3 ML. When compared to the H-bond energy of the gas-phase dimer ( $-130$  meV/ethanol or  $-260$  meV/H-bond), it is found that the H-bonding energy for the adsorbed dimer on Rh(111) is roughly same as in the gas phase. The H-bond energy accounts for 26% of the overall energy gain, and the adsorbate–substrate bonding is dominant for the dimer adsorption in this case.

Although the energy contribution is modest, H-bond has significant effect on OH vibration. For the gas-phase ethanol dimer, the calculated  $\nu(\text{OH})$ 's are  $3618$   $\text{cm}^{-1}$  for the H-donor and  $3862$   $\text{cm}^{-1}$  for the H-acceptor, in contrast to  $3863$   $\text{cm}^{-1}$  for the free monomer. Namely, a red shift of  $\nu(\text{OH})$  at magnitude of  $\sim 245$   $\text{cm}^{-1}$  is produced once the hydroxyl group has been involved into the H-bond. After adsorption, the  $\nu(\text{OH})$  stretches become  $3094$   $\text{cm}^{-1}$  (for the H-donor) and  $3448$   $\text{cm}^{-1}$  (for the H-acceptor) at 2/9 ML, and  $3119$   $\text{cm}^{-1}$  (for the H-donor) and  $3416$   $\text{cm}^{-1}$  (for the H-acceptor) at 1/3 ML. This shows that adsorption results in additional red shift. Furthermore, the red shift for the H-acceptor indicates there is coupling even between the higher-lying ethanol molecule and metal substrate. The overall red shift/softening of  $\nu(\text{OH})$  induced by adsorption and H-bonding for both of the H-donor and H-acceptor has been found to be not less than  $415$   $\text{cm}^{-1}$ . Compared to the ethanol

dimer in gas phase, both of the O–H bonds are elongated by  $\sim 0.02$  Å. For the monomer adsorption (Table 1), the  $\nu(\text{OH})$  red shift  $207$   $\text{cm}^{-1}$  at 1/9 ML is slightly smaller, which correlates well with the less elongation ( $0.01$  Å) of O–H bond length induced by adsorption.

**3.3. One-Dimensional Ethanol Chain.** The adsorbed ethanol dimers can agglomerate further to form one-dimensional (1D) zigzag chain through the H-bond at coverage of 2/9 and/or 1/3 ML, as schematically plotted in Figure 3. As seen from it and Table 3 ( $\Phi$ , the angle between C–C bond and normal direction of the surface), for every second ethanol, its C–C bond is almost perpendicular to the surface, while the C–C bond of the neighbor ethanol is nearly parallel to the surface. In methanol adsorption on Rh(111) surface, similar results have been found, where, instead of the C–C bond, the C–O bond for every second methanol is perpendicular to the surface when the one-dimensional methanol zigzag chain formed.<sup>25</sup> The vertical buckling between the two oxygen atoms are  $0.78$  and  $0.86$  Å at 2/9 and 1/3 ML, which are slightly smaller than the adsorbed dimer at same coverage,  $0.92$  and  $0.96$  Å, respectively. The decreased buckling is because of the enhanced H bonding within the 1D chain.

A distinct feature in the 1D ethanol chain is that all of the hydroxyl groups participate in the H-bond. The lower-lying molecule binds directly to the surface through the O atom, while the higher-lying one forms the H-bond to the lower-lying ethanol molecule in the next unit cell. Each hydroxyl group acts simultaneously as the H-donor and H-acceptor in the zigzag chain. The ratio between the number of the H-bonds to ethanol molecules is 1:1, compared to 1:2 for the adsorbed ethanol dimer, where only one H-bond forms between two adsorbed ethanol molecules. The hydrogen-bonding energy is enhanced roughly by a factor of 2 in the 1D ethanol chain.

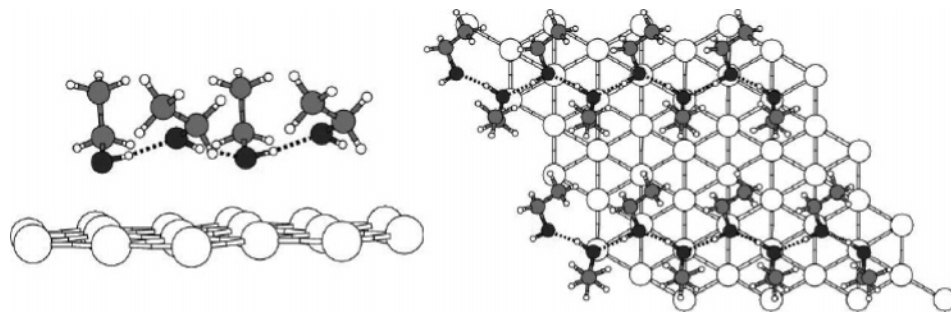


Figure 3. Top view (left) and side view (right) of 1D ethanol chain on Rh(111) surface.

TABLE 3: Averaged Adsorption Energies  $E_{\text{ads}}$ , H Bond Energy  $E_{\text{H-bond}}$  Per Molecule (eV) for 1D Chain Adsorption, and Corresponding Main Structure Parameters (Å and degree), Vibrational Frequencies ( $\text{cm}^{-1}$ ), Variation of Work Function  $\Delta\phi$  (eV), and Surface Dipole Moment  $\mu$  (Debye) at Different Coverage  $\theta$  (ML)

$\Theta$ (ML)	$E_{\text{ads}}$	$E_{\text{H-bond}}$	O-Rh	O-H	$\text{O}_a\text{-O}_b$	C-O	$\Phi$	$\nu_{\text{OH}}$	$\Delta\phi$	$\mu$
2/9	-0.52	-0.328	2.36	1.02	2.67	1.45	7.8	3090	-1.55	1.17
			3.14	1.00	2.79	1.44	68.3	3377		
1/3	-0.50	-0.340	2.36	1.01	2.69	1.45	7.8	3136	-1.80	0.90
			3.22	1.00	2.79	1.44	65.7	3372		

The total energy gain by forming the 1D chain with respect to the dimer adsorption ( $-0.02$  eV/ethanol for coverage of 1/3 and 2/9 ML), however, is small. Therefore, the ratio between the adsorbate-substrate bonding and adsorbate-adsorbate H-bonding to overall energetics has been significantly changed. Using eq 2, the H-bond energy per ethanol molecule is  $-328$  meV (2/9 ML) and  $-340$  meV (1/3 ML), compared to  $-127$  and  $-157$  meV for dimer adsorption, respectively. Specifically, the H-bonding account for roughly 63% of the overall energies at 1/3 ML, contrast to 26% for the dimer adsorption at same coverage. The small variation of the overall energetics for 1D ethanol chain indicates significant weakening of the coupling between 1D ethanol chain and substrate underneath. Finally, we note that the H-bond energy strength (per H-bond) is roughly same for both 1D chain and dimer:  $-328$  meV (2/9 ML) and  $-340$  meV (1/3 ML) for the previous one, and  $-255$  meV (2/9 ML) and  $-315$  meV (1/3 ML) for later one. The dominant role of the H-bonding in the overall energetics for 1D ethanol chain comes simply from increased number of the H-bond.

The O-H vibrations have been affected by formation of the 1D ethanol chain. The calculated  $\nu(\text{OH})$  is  $3090$   $\text{cm}^{-1}$  for the lower-lying molecule and  $3377$   $\text{cm}^{-1}$  for the higher-lying one at coverage of 2/9 ML. With increase of the coverage to 1/3 ML, corresponding vibrations become  $3136$   $\text{cm}^{-1}$  and  $3372$   $\text{cm}^{-1}$ . Compared to the dimer adsorption ( $3094$  and  $3448$   $\text{cm}^{-1}$  for 2/9 ML,  $3119$  and  $3416$   $\text{cm}^{-1}$  for 1/3 ML), the  $\nu(\text{OH})$  of the higher-lying ethanol molecules has been softened further, due to its direct participation into the hydrogen bond, which is otherwise absent for the adsorbed ethanol dimer. The  $\nu(\text{OH})$  for the lower-lying ethanol are less affected because the transition from the dimer to 1D chain mainly change the bonding of the higher-lying ethanol molecules. The overall red shifts for the 1D chain structure with respect to the free ethanol monomer are not less than  $486$   $\text{cm}^{-1}$ .

**3.4. Diagram for Ethanol Adsorption.** The averaged adsorption energies and H-bond energies for the monomer, dimer, or 1D chain adsorption have been plotted in Figure 4. From this figure, it can be found that the overall energy gain from the ethanol adsorption on Rh(111) is exothermic, and the averaged adsorption energy decreases with coverage. Ethanol molecules are energetically favorable to form the dimer via the H-bond between hydroxyl groups, where the H-bonding accounts for roughly 26% of the overall energy gain. The lateral interaction between adsorbed dimers is modest, as seen from

little change of the averaged adsorption energy at the coverage of 2/9 and 1/3 ML. The structure at 1/3 ML will, however, be formed with increasing of the coverage, driven by the thermodynamics. The present calculations indicate that the adsorbed ethanol dimers may rearrange themselves to form 1D chain by forming additional hydrogen bond between adsorbed dimers. Though its overall energetics are very close to the adsorbed dimer, the H-bonding becomes dominant and accounts for about 63% of the overall energy gain with weakened adsorbate-substrate interaction, accordingly.

The formation of the ethanol trimer or tetramer on Rh(111) surfaces within the submonolayer regime, as often found in the hydroxyl liquid or water/solid interfaces, is unlikely in the present case due to the constraint of the metal substrate and large steric repulsion between the adsorbed ethanol molecules. From the present calculations, it can be concluded that the saturation coverage for submonolayer ethanol adsorption on Rh(111) is about 1/3 ML. It will be followed by multilayer growth with further increasing of the coverage. These conclusions may be equally applied to ethanol adsorption on other transition metal surfaces without significant modifications, which do corroborate well with available experimental data. For example, the saturated coverage for the submonolayer ethanol adsorption is 0.2 ML for Ni(111) at 90 K,<sup>12</sup> and 0.44 ML for Pt(111) at 100 K.<sup>18</sup> With increase of the coverage, a multilayer growth of ethanol has been found.<sup>12-24</sup>

As found in the present work, the adsorption results in significant red shift of  $\nu(\text{OH})$  up to  $\sim 500$   $\text{cm}^{-1}$  due to the adsorbate-substrate interaction and the H-bonding between adsorbates. For monomer adsorption at coverage of 1/9 ML, the red shifts of  $\nu(\text{OH})$  is  $207$   $\text{cm}^{-1}$ , which comes solely from the interaction between adsorbed ethanol and Rh(111) by charge depletion in O-H bond (Figure 5a given below). With the coverage increasing and the ethanol dimer formation, overall red shift are not less than  $415$  ( $447$ )  $\text{cm}^{-1}$  at coverage of 2/9 (1/3) ML by the coupling between ethanol molecules and substrate underneath and formation of the hydrogen bond (as indicated in Figure 5b given below). For 1D ethanol chain, the red shift of  $\nu(\text{OH})$  are not less than  $486$  ( $491$ )  $\text{cm}^{-1}$  at 2/9 (1/3) ML though the H-bonding has been enhanced further. Accompanied with above red shifts, the O-H bond length increases correspondingly:  $0.99$  Å (ethanol monomer at 1/9 ML),  $1.01$  Å (ethanol dimer at 2/9 ML), and  $1.02$  Å (1D chain at 2/9 ML). Finally, we note that once the H-bonds are formed either in

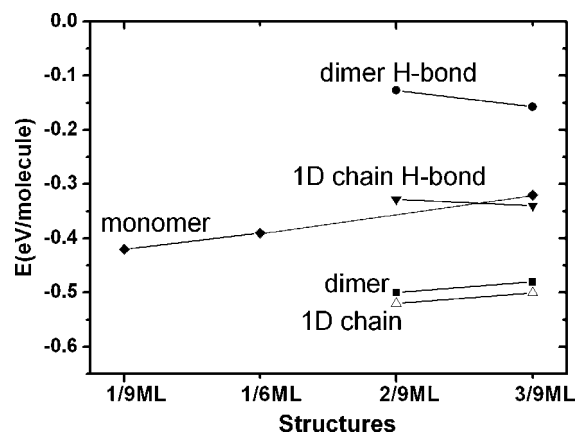


**Figure 4.** Energy diagrams for the averaged adsorption energies (the three lower lines) and H-bond energies per ethanol molecule (the top two lines) for ethanol monomer, dimer, or 1D chain at different coverage.

dimer or 1D chain, there is always a pair of hydroxyl groups involved, with distinct vibrational frequencies, which are different by  $297\text{--}354\text{ cm}^{-1}$  for the adsorbed dimer, and  $232\text{--}287\text{ cm}^{-1}$  for 1D ethanol chain, dependent on the coverage. The existence of the pair of the hydroxyl group and its dependence on the adsorption modes and coverage can be served as the fingerprint of the adsorption structures of ethanol molecules (and even generally the hydroxyl contained molecules like methanol<sup>25</sup> and water<sup>46,47</sup>) and the formation of the H-bonds.

#### 4. Discussion

To best of our knowledge, the formation of H-bond for adsorbed ethanol on metal surfaces has not been well justified, both experimentally and theoretically. Using temperature-programming desorption (TPD) method,<sup>2</sup> King and co-workers studied ethanol adsorption and decomposition on Rh(111) surfaces, and found two ethanol desorption peaks in the temperature range of  $220\text{--}260\text{ K}$ . Isotopic mixing experiments rule out the possibility that the recombination of ethoxide and hydrogen atom produces the parent ethanol molecule, which gives rise to the higher temperature peak. The two TPD peaks have been explained by different ethanol adsorption states, and the higher temperature peak formed with the exposures increase has been attributed to the H-bonds formation between the adsorbed ethanol molecules, which is supported by the present calculations.

As mentioned above, a significant red shift of  $390\text{ cm}^{-1}$  for  $\nu(\text{OH})$  has been observed experimentally after ethanol adsorption on Rh(111).<sup>16</sup> Moreover, for ethanol adsorption on Rh(100), a red shift about  $400\text{ cm}^{-1}$  has been found at high coverages.<sup>14</sup> However, the detailed structures and dependence on the coverage of ethanol adsorption in these studies remain unclear. The present vibrational calculations may shed some lights on this. First, we note that though there is an overestimation of the absolute vibration frequency by  $\sim 5\%$  from the present DFT calculations, the relative shift of the vibrations between different adsorption sites and coverage agree well with experiments largely due to the error cancellation, as found in literatures<sup>48,49</sup> and our previous work.<sup>50</sup> On the basis of the present calculations, it is known that the red shift for  $\nu(\text{OH})$  induced by the monomer adsorption at  $1/9\text{ ML}$  is ca.  $207\text{ cm}^{-1}$ , which is far below the experimental results,  $390\text{ cm}^{-1}$ , and therefore excluded. The monomer adsorption at higher coverage is unlikely as well, since ethanol molecules tend to form dimer or 1D chain. For ethanol

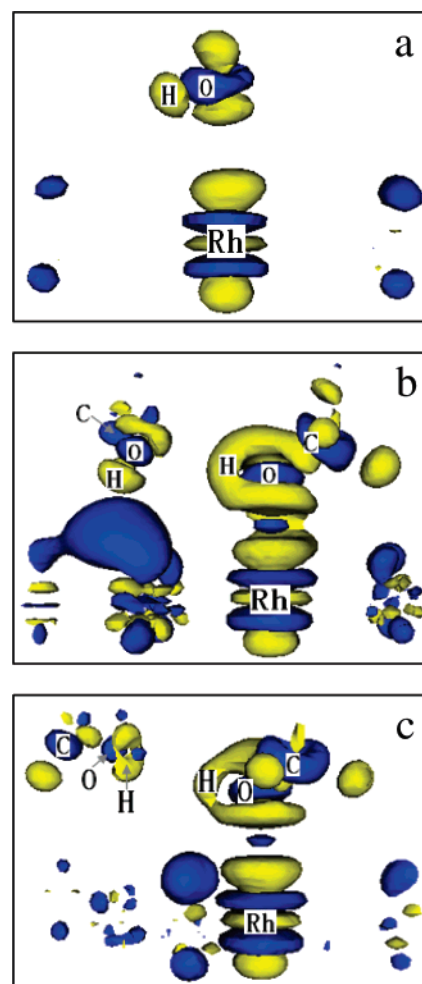


**Figure 5.** Isosurfaces of the difference of electron density for (a) ethanol monomer adsorption, (b) ethanol dimer adsorption, and (c) 1D ethanol chain adsorption. Yellow contours indicate electron depletion, and blue contours indicate electron accumulation. Only atoms with obvious charge transferring are shown for clarity.

adsorption in form of 1D chain, the red shift is at least  $490\text{ cm}^{-1}$ , which is too large and excluded either. For ethanol adsorption in form of a dimer, the red shift of  $\nu(\text{OH})$  from so-called H-acceptor (the higher-lying ethanol molecule) is  $415$  and  $447\text{ cm}^{-1}$  for coverage of  $2/9\text{ ML}$  and  $1/3\text{ ML}$ , which are most close to experimental findings. However, the red shift of  $\nu(\text{OH})$  from so-called H-donor (lower-lying) ethanol has red shift as large as  $769$  and  $745\text{ cm}^{-1}$ , respectively, which were not observed by experiments, and hence the ethanol dimer formation is apparently excluded too. However, by checking the experimental data carefully, we found that there was a peak at  $2990\text{ cm}^{-1}$ , which was attributed to the  $\nu(\text{CH}_3)$ .<sup>16</sup> From our calculations, we know that  $\nu(\text{CH}_3)$  from ethanol,  $\sim 3080\text{ cm}^{-1}$ , which is less perturbed by ethanol adsorption and the dimer formation, is accidentally overlapped with  $\nu(\text{OH})$  for the H-donor within the adsorbed dimer. Therefore, experimental finding at  $2990\text{ cm}^{-1}$ , which was assigned to  $\nu(\text{CH}_3)$  originally, can be equally assigned to the  $\nu(\text{OH})$  from the lower-lying ethanol molecule. With this assignment, the difference between these two vibrations ( $280\text{ cm}^{-1}$ ) found by experiment agrees well with the difference of a pair of  $\nu(\text{OH})$  from the ethanol dimer,  $354\text{ cm}^{-1}$  at coverage  $2/9\text{ ML}$  and  $232\text{ cm}^{-1}$  at coverage  $1/3\text{ ML}$ . On the basis of this discussion, together with their energetics, we conclude that ethanol molecules adsorb on the Rh(111) surface and form ethanol dimer via the H-bond. The

vibration of the 2990  $\text{cm}^{-1}$  found by experiment and assigned to the  $\nu(\text{CH}_3)$  originally is actually from the O–H vibration.

## 5. Electronic Structure Analysis

To illustrate the nature of the interaction between ethanol molecules and the Rh(111) surfaces, their electronic structures are analyzed in this section. To do this, the difference of electron density of adsorbate–substrate system are plotted in Figure 5 using the formula given below:

$$\rho(\text{Rh} + \sum \text{ethanol}) - \rho(\text{Rh}) - \sum \rho(\text{ethanol}) \quad (3)$$

where  $\rho(\text{Rh} + \sum \text{ethanol})$  is the electron density of the adsorbate–substrate system and  $\rho(\text{Rh})$  and  $\sum \rho(\text{ethanol})$  are the electron density of the substrate and the isolated adsorbates frozen at the geometries in the combined system, respectively. For monomer adsorption (Figure 5a), it can be found that the adsorption induces pronounced electron transfer from the H atom of the OH group to oxygen, and polarization of Rh atom underneath. The difference of electron density for dimer adsorption is plotted in Figure 5b. With the directional H-bond formation, the electron along the H-bond has been polarized further. This polarization has been enhanced for 1D ethanol chain. Accordingly, adsorption induced electronic perturbation toward the substrate decreases, and coupling between the adsorbates and substrate has been weakened. These are in line with the energetics found in above, where the H-bonding becomes dominant for the 1D chain adsorption.

The charge transfer between adsorbate and substrate can be seen further from the reduction of work function (larger than 1.28 eV), as shown in Tables 1–3. The work function decreases with the coverage, which indicates the continuous charge accumulation into the substrate. The amount of charge transferred per ethanol molecule, however, decreases due to the depolarization, which can be characterized by so-called surface dipole moment  $\mu$  (in Debye, and tabulated in Tables 1 and 2), calculated by

$$\mu = \frac{1}{12\pi} A \frac{|\Delta\varphi|}{\theta} \quad (4)$$

where  $\Delta\varphi$  is the variation of the work function,  $A$  is the area per ( $1 \times 1$ ) surface unit cell, and  $\theta$  is the coverage. For monomer adsorption on Rh(111) surface,  $\mu$  decreases from 1.93 Debye (1/9 ML) to 1.04 Debye (1/3 ML), while it decreases from 1.03 Debye (2/9 ML) to 0.85 Debye (1/3 ML) for dimer adsorption. The depolarization with the coverage indicates the decrease of the charge-transfer per ethanol molecule, which minimizes the electrostatic repulsion between the adsorbates. Compared to the variation of the work function ( $-2.07$  eV) and dipole moment (1.04 Debye) for monomer adsorption at 1/3 ML, smaller reduction of work function ( $-1.70$  eV) and dipole moment (0.85 Debye) for the ethanol dimer at same coverage provides the driven forces for the formation of the H-bond. Though there is no experimental data available for this particular system, the reduction of the work function with increase of the coverage for methanol adsorption on Rh(100) surfaces have been reported by Parmeter et al.<sup>38</sup>

## 6. Conclusions

The adsorptions of ethanol on Rh(111) surface within the submonolayer regime are studied systematically by density functional theory in the present work. Some of the key findings and implications are summarized below:

(i) Ethanol molecule adsorption is exothermic and prefers the atop of sites by binding to the surface via its oxygen atom. This site preference exhibits little dependence on coverage and adsorption mode, e.g., monomer, dimer, and chain. The interaction between ethanol and the metal substrate, however, is modest, and the average adsorption energy is about  $-0.5$  eV. It is found that adsorbed ethanol molecules tend to agglomerate to dimer and chain by formation of the hydrogen bond. For adsorbed dimer, the adsorbate–substrate interaction is dominant, and the H-bond energy ( $\sim 130$  meV per ethanol molecule or 260 meV per H-bond) accounts for only 26% of the overall energetics. For chain structures, more hydrogen bonds are formed, and the H-bond energy increases to 63%, accompanied with weakening of the adsorbate–substrate interaction. The saturated coverage for ethanol adsorption on Rh(111) (more generally to close-packed transition metal surfaces) is predicted to be  $\sim 1/3$  ML within submonolayer regime.

(ii) Ethanol adsorption and agglomeration into the dimer and 1D chain structures have significant effects on the OH vibration. It is found that the red shifts of the OH vibration are very sensitive to the adsorption structures and the types of the interactions between adsorbate and the substrate as well as the H-bonding between the adsorbed ethanol molecules. Our results show that these two kinds of interaction result in the overall red shift of  $\nu(\text{OH})$  to the magnitude of  $769$   $\text{cm}^{-1}$ , which is accidentally overlapped with the  $\nu(\text{CH}_3)$ . The present study indicates that the existence of the distinct pair of OH vibrations can be used as the fingerprint for alcohol adsorption modes and the formation of the H-bond.

**Acknowledgment.** W.X.L. gratefully acknowledges financial support from the National Natural Science Foundation of China (No. 20503030) and Chinese Academy of Sciences “Bairen Project”. X.H.B. thanks the financial support from the National Natural Science Foundation of China (No. 90206036) and the Ministry of Science and Technology of China (2005CB221405). The authors thank Jason White from UCSB for reading through the manuscript.

## References and Notes

- Deluga, G. A.; Salge, J. R.; Schmidt, L. D.; Verykios, X. E. *Science* **2004**, *303*, 993.
- Papageorgopoulos, D. C.; Ge, Q.; King, D. A. *J. Phys. Chem.* **1995**, *99*, 17645.
- Laenen, R.; Rauscher, C. *J. Chem. Phys.* **1997**, *107*, 9759.
- Lalanne, P.; Andanson, J. M.; Soetens, J. C.; Tassaing, T.; Danten, Y.; Besnard, M. *J. Phys. Chem. A* **2004**, *108*, 3902.
- Murdoch, K. M.; Ferris, T. D.; Wright, J. C.; Farrar, T. C. *J. Chem. Phys.* **2002**, *116*, 5717.
- Peeters, D.; Leroy, G. *J. Mol. Struct. (THEOCHEM)* **1994**, *314*, 39.
- Buck, U.; Huisken, F. *Chem. Rev.* **2000**, *100*, 3863.
- Guo, J.-H.; Luo, Y.; Augustsson, A.; Kashtanov, S.; Rubensson, J.-E.; Shuh, D. K.; Ågren, H.; Nordgren, J. *Phys. Rev. Lett.* **2003**, *91*, 157401.
- Takahashi, H.; Hashimoto, H.; Nitta, T. *J. Chem. Phys.* **2003**, *119*, 7964.
- Coussan, S.; Roubin, P.; Perchard, J. P. *J. Phys. Chem. A* **2004**, *108*, 7331.
- George, W. O.; Has, T.; Hossain, Md. F.; Jones, B. F.; Lewis, R. *J. Chem. Soc., Faraday Trans.* **1998**, *94*, 2701.
- Xu, J. Z.; Zhang, X. P.; Zenobi, R.; Yoshinobu, J.; Xu, Z.; Yates, J. T., Jr. *Surf. Sci.* **1991**, *256*, 288.
- Kartochwil, T.; Wittmann, M.; Kuppers, J. J. *Electron Spectrosc. Relat. Phenom.* **1993**, *64–65*, 609.
- Tian, Z.-J.; Wei, X.-M.; Zhai, R.-S.; Ren, S.-Z.; Liang, D.-B.; Lin, L.-W. *Chem. J. Chin. Univ.* **1997**, *7*, 1153.
- Mavrikakis, M.; Barteau, M. A. *J. Mol. Catal., A* **1998**, *131*, 135.
- Houtman, C. J.; Barteau, M. A. *J. Catal.* **1991**, *130*, 528.
- Vesselli, E.; Baraldi, A.; Comelli, G.; Lizzit, S.; Rosei, R. *ChemPhysChem* **2004**, *5*, 1133.

- (18) Lee, A. F.; Gawthorpe, D. E.; Hart, N. J.; Wilson, K. *Surf. Sci.* **2004**, *548*, 200.
- (19) Rajumon, M. K.; Roberts, M. W.; Wang, F.; Wells, P. B. *J. Chem. Soc., Faraday Trans.* **1998**, *94*, 3699.
- (20) Alcalá, R.; Mavrikakis, M.; Dumesic, J. A. *J. Catal.* **2003**, *218*, 178.
- (21) Cong, Y.; van Spaendonk, V.; Masel, R. I. *Surf. Sci.* **1997**, *385*, 246.
- (22) Cong, Y.; Masel, R. I. *Surf. Sci.* **1998**, *396*, 1.
- (23) Holroyd, R. P.; Bennett, R. A.; Jones, I. Z. *J. Chem. Phys.* **1999**, *110*, 8703.
- (24) Davidson, J. M.; McGregor, C. M. *Indus. Eng. Chem. Res.* **2001**, *40*, 108.
- (25) Koch, H. P.; Krenn, G.; Bako, I.; Schennach, R. *J. Chem. Phys.* **2005**, *122*, 244720.
- (26) Schennach, R.; Eicher, A.; Rendulic, K. D. *J. Phys. Chem. B* **2003**, *107*, 2552.
- (27) Houtman, C. J.; Barteau, M. A. *Langmuir* **1990**, *6*, 1558.
- (28) Neurock, M. *Top. Catal.* **1999**, *9*, 135.
- (29) Desai, S. K.; Neurock, M.; Kourtakis, K. *J. Phys. Chem. B* **2002**, *106*, 2559.
- (30) Ge, Q.; Desai, S. K.; Neurock, M. *J. Phys. Chem. B* **2001**, *105*, 9533.
- (31) Greeley, J.; Mavrikakis, M. *J. Am. Chem. Soc.* **2002**, *124*, 7193.
- (32) Remediakis, I. N.; Abild-Pedersen, F.; Nørskov, J. K., *J. Phys. Chem. B* **2004**, *108*, 14535.
- (33) Greeley, J.; Mavrikakis, M. *J. Catal.* **2002**, *208*, 291.
- (34) Branda, M. M.; Ferullo, R. M.; Belelli, P. G.; Castellani, N. *J. Surf. Sci.* **2003**, *527*, 89.
- (35) Wang, G. C.; Zhou, Y. H.; Morikawa, Y.; Nakamura, J.; Cai, Z. S.; Zhao, X. Z. *J. Phys. Chem. B* **2005**, *109*, 12431.
- (36) Chen, J. J.; Jiang, Z. C.; Zhou, Y.; Chakraborty, B. R.; Winograd, N. *Surf. Sci.* **1995**, *328*, 248.
- (37) Francis, S. M.; Corneille, J.; Goodman, D. W.; Bowker, M. *Surf. Sci.* **1996**, *364*, 30.
- (38) Parmeter, J. E.; Jiang, X.; Goodman, D. W. *Surf. Sci.* **1990**, *240*, 85.
- (39) Hammer, B.; Hansen, L. B.; Nørskov, J. K. *Phys. Rev. B* **1999**, *59*, 7413.
- (40) Perdew, J. P.; Chevary, J. A.; Vosko, S. H.; Jackson, K. A.; Pederson, M. R.; Singh, D. J.; Fiolhais, C. *Phys. Rev. B* **1992**, *46*, 6671.
- (41) Neugebauer, J.; Sheffler, M. *Phys. Rev. B* **1992**, *46*, 16067.
- (42) Delbecq, F.; Vigné, F. *J. Phys. Chem. B* **2005**, *109*, 10797.
- (43) Görbitz, C. H. *J. Mol. Struct. (THEOCHEM)* **1992**, *262*, 209.
- (44) Ludwig, R.; Weinhold, F.; Farrar, T. C. *Mol. Phys.* **1999**, *97*, 465.
- (45) Sexton, B. A. *Surf. Sci.* **1979**, *88*, 299.
- (46) Meng, S.; Xu, L. F.; Wang, E. G.; Gao, S. W. *Phys. Rev. Lett.* **2002**, *89*, 176104.
- (47) Meng, S.; Wang, E. G.; Gao, S. W. *Phys. Rev. B* **2004**, *69*, 195404.
- (48) Neurock, M. In *Catalytic Surface Reaction Pathways and Energetics from First Principles*; Froment, G. F., Waugh, K. C., Eds.; Press: Elsevier Science: Amsterdam, 1997.
- (49) Neurock, M. *J. Catal.* **2003**, *216*, 73.
- (50) Yang M. M.; Bao, X. H.; Li, W. X. Unpublished results, 2007.